Solar Thermochemical Water-Splitting for H_2 Generation Using Sol-Gel Derived Ferrite Nanomaterials

R. R. Bhosale, X. Pasala, S. Yelakanti, J. A. Puszynski, R. V. Shende*

Chemical and Biological Engineering,
South Dakota School of Mines and Technology,
Rapid City, SD 57701. Rajesh.Shende@sdsmt.edu

ABSTRACT

This Paper reports sol-gel synthesis of Ni-ferrite and Zn-doped Ni-ferrite materials, which involved the addition of metal salt precursors in ethanol followed by gelation using propylene oxide. As-prepared gels were aged for 24 hrs, calcined at 600^{o}C and cooled rapidly in air environment. In addition, Ni-ferrite/ YSZ (yttria-stabilized zirconia) powdered material was also prepared using a vortex mixer. These powdered ferrite materials were analyzed using scanning electron microscopy (SEM), X-ray diffraction (XRD) and BET (Brunauer-Emmett-Teller) surface area analyzer. The H_2 generation ability of these ferrite nanomaterials was investigated by performing four consecutive thermochemical cycles in the Inconel packed-bed reactor where water-splitting and regeneration were carried out at 700-900^{o}C and 1100^{o}C, respectively. The use of YSZ was found to mitigate the grain growth of ferrite particles and affected the H_2 volume generation.

Keywords: Ni-ferrite, Zn-doped Ni-ferrite, Ni-ferrite/YSZ powdered mixture, sol-gel, water-splitting, H_2 generation.

1. INTRODUCTION

H_2 is a green fuel with higher energy density as compared with the fossil fuels. Industrially H_2 is produced via fossil fuel steam reforming process as it is economical as compared with other production processes. Although this process is significantly cost-effective it leads to CO_2 emission, which is believed to have some impact on global warming. Thermochemical water-splitting process using redox materials is one of the green processes for H_2 production [1]. This process has a two-step approach; where in step-1, partially reduced metal oxide ($MO_{reduced}$) is reacted with steam leading to H_2 formation and in step-2, oxidized metal oxide ($MO_{oxidized}$) is regenerated at higher temperature converting back to its reduced form ($MO_{reduced}$). Together one water-splitting step (1) and one regeneration step (2) is referred as one thermochemical cycle [2]. Typically water-splitting step can be performed at lower temperatures; however, regeneration of redox materials requires higher temperatures. When a redox material is heated at higher temperatures, oxygen vacancies are created leading to the formation of non-stoichiometric metal oxide [3]. When such a material is contacted with the steam, it scavenges the oxygen leading to H_2 generation as per the following exothermic reaction-

$$MO_{reduced} + H_2O \xrightarrow{\Delta} MO_{oxidized} + H_2 \qquad (1)$$

The $MO_{oxidized}$ is further reduced in inert environment by releasing the O_2 at high temperatures in the endothermic regeneration step-

$$MO_{oxidized} \xrightarrow{\Delta} MO_{reduced} + \tfrac{1}{2}\, O_2 \qquad (2)$$

Overall thermochemical water-splitting process is very attractive because H_2 and O_2 are generated in two different steps avoiding the possibility of explosive mixture formation. The cyclic nature of the process, however, leads to higher process downtime because of the temperature swing operation. One of the greater challenges in this process is to reduce the water-splitting and regeneration temperatures so that the solar concentrator technology can be effectively utilized for sustainable H_2 production. Therefore, there is a need to develop novel redox materials capable of performing water-splitting reaction at lower temperatures.

Among several redox materials, ferrites show higher H_2 volume generation at lower temperatures. Several nominally phase pure ferrite materials have been investigated for H_2 generation from water-splitting reaction. Further enhancement in water-splitting capacity of ferrites can be achieved if higher O_2 vacancies are created in crystal lattices. It is believed that the doping of the phase pure ferrite materials with bivalent metals can increase O_2 vacancies. In addition to nominally phase pure ferrite, several doped ferrites such as Ni-Mn ferrite, Ni-Zn ferrite, Mn-Zn ferrite, Cu-Zn ferrite and Cu-Mn ferrite [4-9] were also investigated for water-splitting application. Many investigators reported synthesis of doped and undoped ferrites using solid-state synthesis (SSS), oxidation of aqueous metal hydroxide suspension, self-propagation high temperature synthesis (SHS) and aerosol-spray pyrolysis (ASP). These synthesis methods excluding the ASP show the characteristics of chemical heterogeneity, non-stoichiometry and non-porous morphology leading to lower SSA [2, 10,11]. When such a

Cleantech 2012, www.ct-si.org, ISBN 978-1-4665-6277-6

material is used for water-splitting application in a packed-bed reactor configuration, O_2 scavenging can occur only on the external surface of reduced ferrite material. In addition, possible transport of oxygen up to the core may not be achieved. Consequently, lower H_2 volume generation will be realized. Under such a situation one option will be to increase water-splitting and regeneration temperature but such efforts will induce thermal stresses in ferrite materials leading to sintering and grain growth.

The ferrites prepared using sol-gel method will have the characteristics of molecular and atomic level mixing and networking of chemical components, chemical homogeneity, desired stoichiometry, phase purity and nanoparticle morphology with high specific surface area. Over the period of last three years, we synthesized several ferrite materials using sol-gel technique and these materials showed characteristic SSA of 10-35 m^2/g, crystallite size of about 20-40 nm and higher pore volume based on the calcination conditions employed. Higher SSA provides higher active sites whereas with nanoparticle morphology the diffusional and mass transfer limitations can be minimized. When sol-gel derived Ni-ferrite material with nanoparticle morphology was used for thermochemical water-splitting, a significant grain growth was observed [12] leading to SSA < 1 m^2/g. This obviously reduced the H_2 volume generation in additional thermochemical cycles. The grain growth and sintering of redox materials and decrease in H_2 production has also been observed by other investigators [13]. Thus it appears that there exists a greater challenge on the process front as how to mitigate the grain growth or sintering during thermal cycling operation.

In this paper we report sol-gel synthesis of Zn-doped Ni-ferrite and preparation of Ni-ferrite/YSZ powdered mixture. These materials were characterized and used for H_2 generation at 700°-900°C from water-splitting reaction.

2. EXPERIMENTAL

2.1 Synthesis of Ni-doped Ferrites

For Zn-doped Ni-ferrite, $NiCl_2$. $6H_2O$, $ZnCl_2.4H_2O$ and $FeCl_2.4H_2O$ (0.44:0.37:1 w/w ratio) were added in 20 ml of ethanol and sonicated to obtain a visually clear solution. To this solution, propylene oxide was added to achieve the gel formation. As prepared gel was aged for 24 hrs and dried on hot plate at 100°C for about 1 hr and this dried powder was calcined up to 600°C in a muffle furnace at a ramp rate of 40°C/min and rapidly cooled in air environment. To prepare Ni-ferrite/YSZ powdered mixture, the YSZ (25 wt %) was added to the calcined Ni-ferrite and mixed together using vortex mixer for about 15 min.

2.2 Characterization of Ferrites

These calcined ferrites were analyzed using X-ray diffraction (Rigaku Ultima-plus X-ray diffractometer with scanning speed of 2° per minute and $10^o \leq 2\theta \leq 70^o$). The particle morphology was analyzed by using scanning electron microscope (Zeiss Supra 40 VP field-emission) and transmission electron microscope. The SSA of the ferrites was determined by using BET surface area analyzer (Gemini II – 2375).

2.3 Hydrogen Generation Set-Up

The schematic of H_2 generation set-up is shown in the Figure 1. It consists of a tubular packed bed reactor enclosed in a vertical split furnace. The temperature of the furnace was controlled and regulated precisely with the in-built PID controller. Accurately weighed 5.0 g of the ferrite material was packed in the middle section of the tubular reactor using Raschig rings and quartz wool as support for the ferrite materials.

A horizontal tube furnace was provided with a stainless steel tube (O.D. = 0.75 inch and I.D. = 0.634 inch) and it was used as a water vaporizing/preheating set-up. Distilled water from the reservoir was fed to the vaporizing/preheating furnace using a metering pump at the flow rate of 1 mL/min. Water vaporized and the preheated steam obtained was fed to the packed-bed reactor with N_2 as a carrier gas. A mass flow meter for N_2 was mounted on the feed line to control the carries gas flow rate; a flow rate of about 100SCCM/min was randomly selected. The water-splitting ability of Zn-doped Ni-ferrite and Ni ferrite/YSZ powdered mixture were determined by performing four consecutive thermochemical cycles where water-splitting and regeneration steps were performed at 700-900°C and 1100°C, respectively. The exit gas stream of N_2 and H_2 during the water-splitting step was continuously monitored using an online H_2 sensor HY-OPTIMA 730 from H_2 Scan Corp., USA. The sensor read the H_2 concentration in vol% at an interval of 1 sec. The water supply was shut off when the H_2 sensor indicated 0.95vol % concentration.

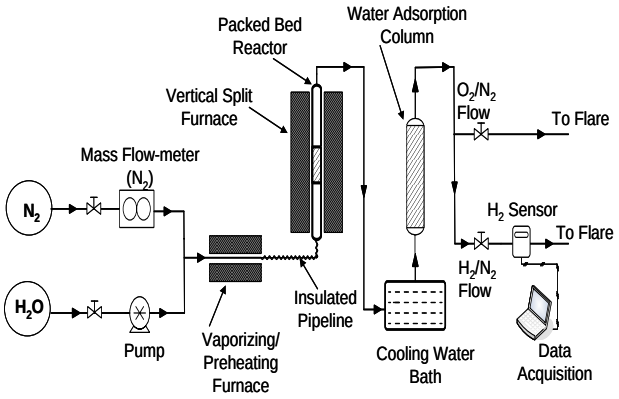

Figure 1: Thermochemical water-splitting reactor set-up for H_2 generation [13].

3. RESULTS AND DISCUSSIONS

3.1 Synthesis of doped Ni-ferrites

As-prepared Zn-doped Ni-ferrite gels were dried and calcined at 600°C in air or N_2 environment. Figure 2 shows XRD profile obtained for Zn-doped Ni-ferrite calcined in air environment at temperatures of 600°-900°C. The XRD analysis of the gels calcined in air indicated a phase composition of $Ni_{0.5}Zn_{0.5}Fe_2O_4$ whereas those calcined in N_2 environment showed a mixed phase composition containing 80% $Ni_{0.5}Zn_{0.5}Fe_2O_4$ and 20% Ni. In general the peak broadening was noticed at 600°C indicating the amorphous nature [14].

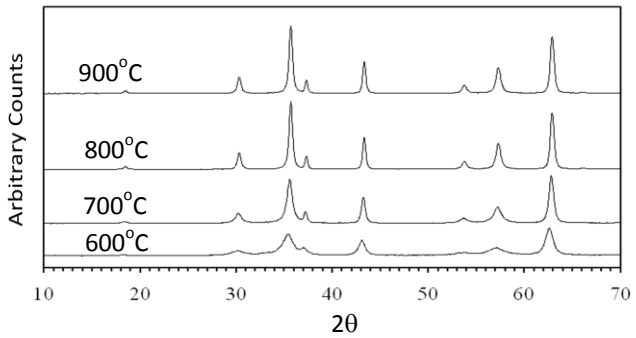

Figure 2: XRD patterns of Zn-doped Ni-ferrite calcined at different temperatures in air environment.

From the BET surface area analysis results, it was observed that the SSA and pore volume decrease and crystallite size increases with increase in the calcination temperature in both air and N_2 environments. At 600°C calcination temperature, SSA of 35 m^2/g, pore volume of 0.063 cm^3/g and crystallite size of 22.5 nm was observed. At 900°C, however, the SSA decreased to about 10 m^2/g and the crystallite size increased to 42 nm. The SEM and TEM images of Ni-Zn-ferrite powders obtained after rapid calcination of the dried gels up to 600°C in air environment are shown in Figures 3a and 3b. The SEM image indicates foam-like porous morphology whereas the TEM image confirms the formation of nanosize Ni-Zn-ferrite particles.

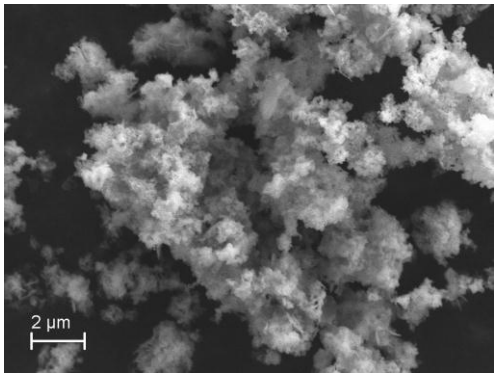

Figure 3a): SEM image of Zn-doped Ni-ferrite gels rapidly calcined up to 600°C and quenched in air.

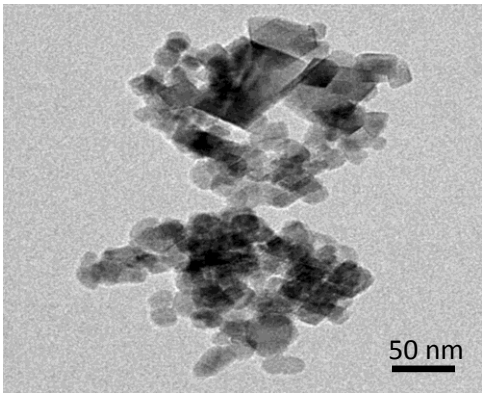

Figure 3b): TEM image of Zn-doped Ni-ferrite gel rapidly heated up to 600°C and quenched in air environment.

Ni-ferrite/YSZ powdered mixture was prepared by the addition of YSZ nanoparticles (25 wt %) to the sol-gel derived Ni-ferrite followed by vortex mixing for 15 min. The phase composition, SSA and morphology of the powdered mixtures were analyzed using powder X-ray diffractometer, BET surface area analyzer, SEM and EDX. The XRD pattern indicated 2θ reflections corresponding to Ni-ferrite and YSZ consistent with ICDD patterns (data not included). The SSA was in the range of 34-37 m^2/g. The EDX analysis showed non-homogenous distribution of YSZ in Ni-ferrite, which was obvious as the powders were mixed for 15 min without any optimization.

3.2 H_2 generation

The H_2 generation ability of these ferrite materials was performed in four thermochemical cycles. The water-splitting temperature for Zn-doped Ni-ferrite was selected as 900°C whereas for Ni-ferrite/YSZ powdered mixture 700°C was used. In both cases, however, the regeneration temperature of 1100°C was employed. From the transient H_2 profiles obtained during four thermochemical cycles for Zn-doped Ni-ferrite and Ni-ferrite/YSZ powdered mixture, average H_2 volume was calculated and it is presented in Table 1.

Material	T_{ws}, °C	H_2 (mL/g) Cycle				Avg H_2, mL/g
		1st	2nd	3rd	4th	
Ni-Ferrite	700	17.3	5.9	4.8	3.5	7.9
Ni-Zn-Ferrite	900	15.3	7.7	5.2	3.9	8.0
Ni-ferrite/YSZ	700	18.9	6.8	6.3	5.6	9.4

Table 1: H_2 volume generated during four thermochemical cycles performed using Zn-doped Ni-ferrite and Ni-ferrite/YSZ powdered mixture.

From the results presented in Table 1, the average H_2 volume generated with Zn-doped Ni-ferrite at 900^{o}C water-splitting temperature was about 8 ml/g/cycle. The H_2 volume generation was found to be maximum for Ni-ferrite/YSZ powdered mixture as compared with Ni-ferrite and Zn-doped Ni-ferrite, which indicates that YSZ played a role in mitigating the grain growth. In absence of Ni-ferrite, YSZ alone, however, did not show any H_2 generation. To validate whether or not YSZ has mitigated the grain growth, the ferrite powdered mixtures obtained after the thermochemical waters-splitting reaction were analyzed using SEM.

The SEM analysis of the reacted Ni-ferrite and Ni-ferrite/YSZ (Figure 4) indicated heterogeneous grain growth. For Ni-ferrite/YSZ powdered mixture, for fewer grains, the grain size of 1–3 μm was observed. Additionally, grains in the size range of 200 – 500 nm were also observed. In contrast to this, the SEM image of the Ni-ferrite material obtained after performing four thermochemical cycles at similar operating conditions indicated larger grain size in the range of 2 to 10 μm. The comparison between the SEM images of the reacted powdered mixtures and the Ni-ferrite material after performing four thermochemical cycles indicated inhibition in the grain growth due to the addition YSZ nanoparticles to the ferrite material.

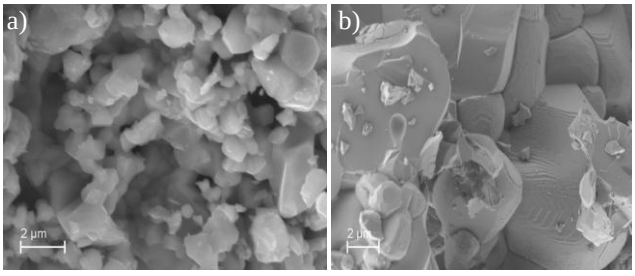

Figure 4: SEM images of a) Ni-ferrite/YSZ and b) Ni-ferrite after performing four thermochemical cycles.

4 CONCLUSIONS

Sol-gel derived Zn-doped Ni-ferrite after calcination in air at 600^{o}C yielded $Ni_{0.5}Zn_{0.5}Fe_2O_4$ with SSA of about 35 m^2/g. When Ni-ferrite was mixed with YSZ nanoparticles using vortex mixing, a non-homogeneous distribution of YSZ in Ni-ferrite/YSZ powdered mixture was evident during EDX analysis. Among the three ferrite materials investigated here, Ni-ferrite/YSZ powdered mixture provided highest H_2 volume generation of avg. 9.4 ml/g/cycle in four consecuative thermochemical cycles where water-splitting and regeneration were performed at 700^{o}C and 1100^{0}C, respectively. The SEM analysis of the ferrites that underwent four thermochemical cycles revealed that YSZ have effect on mitigating the grain growth. In the case of reacted Ni-ferrite material, the particles were found to be in the range of 2-10 μm whereas for Ni-ferrite/YSZ powdered mixture, heterogeneous growth was observed with particles size ranging from 200-500 nm and 1-3 μm. These result suggest that grain growth mitigation or thermal stabilization of ferrite materials will lead to higher and steady H_2 volume generation in multiple thermochemical cycles.

ACKNOWLEDGEMENTS

The authors gratefully acknowledge the financial support by the National Science Foundation, Grant Nos. CBET-0756214, CBET-1134570 and the Chemical and Biological Engineering Department at the South Dakota School of Mines and Technology.

REFERENCES

[1] M. Neises, M. Roeb, M. Schmucker, C. Sattler and R. Pitz Paal, International Journal of Energy Research. 34, 652, 2009.

[2] Steinfeld A, Kuhn P, Reller A, Palumbo R, Murray J, Tamaura Y. International Journal of Hydrogen Energy, 23, 767, 1998.

[3]C. Agrafiotis, C. Pagkoura, S. Lorentzou, M. Kostoglou and A. Knostandopoulos, Catalysis Today, 127, 265, 2007.

[4] R. R. Bhosale, R. V. Shende, J. A. Puszynski, International Review of Chemical Engineering 2, 852, 2010.

[5] R.V. Shende, J.A. Puszynski, M.K. Opoku, R.R. Bhosale, In: Proceedings of NSTI – Nanotech Conference & Expo., ISBN 978-1-4398-1782-7; 2009 May 3 – 7; Houston, TX, USA.

[6] M. Inoue, N. Hasegawa, R. Uehara, N. Gokon, H. Kaneko, Y. Tamaura, Solar Energy, 76, 309, 2004.

[7] Y. Tamamura, Energy, 20, 325, 1995.

[8] S. Lorentzou, C. Agrafiotis, A.G. Konstandopoulos, Granular Matter, 10, 113, 2008.

[9] F. Fresno, R. Fernandez-Saavedea, M.B. Gomez-Mancebo, A. Vidal, M. Sanchez, M.I. Rucandio MI, International Journal of Hydrogen Energy, 34, 2918, 2009.

[10] R. Bhosale, R. Shende and J. Puszynski, AIChE Annual Meeting. November 7-12; Salt Lake City, UT, USA, 2010

[11] R. Bhosale, R. Shende and J. Puszynski, International Journal of Hydrogen Energy, 37, 2924, 2012.

[12] R.R. Bhosale, R.V. Shende, J.A. Puszynski, In: Proceedings of MRS Fall Meeting, 2011; November 28- December 2, Boston, MN, USA.

[13] T. Kodama, N. Gokon, R. Yamamoto, Solar Energy 82, 73, 2008.

[14] R. Bhosale, R. Shende and J. Puszynski, Journal of Energy and Power Engineering. 4, 27, 2010.